Journal of Physiology (1989), **413**, *pp.* 255–269
With 5 text-figures
Printed in Great Britain

DENDRITES OF CAT'S SPINAL MOTONEURONES: RELATIONSHIP BETWEEN STEM DIAMETER AND PREDICTED INPUT CONDUCTANCE

BY D. KERNELL AND B. ZWAAGSTRA

From the Department of Neurophysiology, University of Amsterdam, Academisch Medisch Centrum, Meibergdreef 15, 1105 AZ Amsterdam, The Netherlands

(*Received 20 July 1988*)

SUMMARY

1. The electroanatomy of motoneuronal dendrites was analysed using data from fifty-two dendritic trees of four completely reconstructed cat spinal motoneurones that had been labelled with intracellularly injected horseradish peroxidase. The cells belonged to m. triceps surae, and their physiological properties covered much of the known range for this muscle.

2. For each dendritic tree, the input conductance, as seen from the soma, was calculated by the method of Rall (1959), using anatomical measurements of the length and diameter of all branches and different assumed values for dendritic membrane resistivity.

3. There was a strong positive correlation between dendritic stem diameter and the calculated dendritic input conductance. Dendritic input conductance was approximately equal to a constant $\times$ (stem diameter)$^{3/2}$ $\times$ (dendritic membrane resistivity)$^{-0.76}$.

4. The relationship between dendritic stem diameter and computed input conductance was equal to that of Rall's equivalent-cylinder model of a dendritic tree. However, from a number of other points of view, the properties of the reconstructed dendrites differed from those of the model: (a) at branch points, the sum Σ(daughter diameters$^{3/2}$) was, on average, 19% greater than the 3/2 power of the parent diameter; (b) dendritic branches often showed a significant amount of tapering, and the mean overall degree of diameter decrease per branch was about 12%; (c) the termination of dendritic branches occurred at widely different distances from the soma within single dendritic trees (true for anatomical as well as for computed electrotonic distances).

5. When used in conjunction with previously published measurements of motoneuronal input resistance and proximal anatomy (Kernell & Zwaagstra, 1981), the present results gave further support to the conclusion that differences in membrane resistivity are of great importance for differences in motoneuronal input resistance. Furthermore, this conclusion was also confirmed by direct observation of the properties of the present four motoneurones: irrespective of the assumed ratio between somatic and dendritic membrane resistivity, there was a statistically significant positive correlation between the measured neuronal input resistance and the required membrane resistivity of soma and dendrites.

INTRODUCTION

There are large and physiologically important differences between different functional classes of spinal hindlimb motoneurones with respect to their neuronal input conductance (e.g., Kernell, 1966; Burke & ten Bruggencate, 1971; Kernell & Zwaagstra, 1981; Burke, 1981; Burke, Dum, Fleshman, Glenn, Lev-Tov, O'Donovan & Pinter, 1982; Gustafsson & Pinter, 1984; Ulfhake & Kellerth, 1984). Among such neurones, the dendritic surface area is about 30 or more times greater than that of the cell body (Ulfhake & Kellerth, 1981, 1984; Cullheim, Fleshman, Glenn & Burke, 1987). It is a matter of recent discussion to what extent the passive membrane properties of motoneuronal dendrites differ from those of the soma (Iansek & Redman, 1973; Fleshman, Segev, Cullheim & Burke, 1983; Ulfhake & Kellerth, 1984; Clements & Redman, 1986; Glenn, Samojla & Whitney, 1987). However, in the case of uniform membrane properties, the input conductance of a motoneurone would clearly be expected to be determined, to an important degree, by the properties of its dendrites. The input conductance of a dendrite depends on its specific membrane resistivity as well as on its size and branching pattern. Hence, for a given value of resistivity, an accurate estimate of dendritic input conductance could only be obtained by reconstructing and measuring the whole dendritic tree. Such reconstructions, measurements and calculations are complex and highly time consuming (Rall, 1959). Therefore, it has been of interest to try to predict the electrophysiological properties of dendrites from more limited kinds of measurement.

Rall (1959, 1977) has demonstrated that there is a class of dendritic trees whose electrical behaviour, as seen from the soma, conforms to that of a simple uniform cylinder with a finite length. For such a uniform membrane cylinder, the input conductance is proportional to the 3/2 power of the (stem) diameter. In a preceding study we made use of this hypothetical relationship between stem diameter and dendritic input conductance in an electroanatomical analysis of spinal motoneurones (Kernell & Zwaagstra, 1981). There exists, however, a considerable amount of uncertainty concerning the extent to which the detailed anatomy of motoneuronal dendrites actually agrees with the class of dendritic trees that can, from electrophysiological points of view, be viewed as a uniform cylinder. For the ideal 'equivalent-cylinder dendrite' of Rall (1959, 1977), the required anatomy is such that: (a) at each branch-point, the ratio Σ(daughter branch diameters$^{3/2}$)/(parent branch diameter$^{3/2}$) (i.e. the $D32$ branch-point ratio) equals 1·0; (b) there is no tapering of dendritic branches; (c) all terminal branches end at the same electrotonic distance from the soma.

In preceding quantitative studies of the dendrites of intracellularly labelled hindlimb motoneurones, the average $D32$ branch-point ratios have generally been found to be highly variable, and average values have been reported to be close to 1·0 (Lux, Schubert & Kreutzberg, 1970; Ulfhake & Kellerth, 1981, 1983, 1984; Brown & Fyffe, 1981) or tended to be greater than 1·0 (Egger & Egger, 1982; Cullheim *et al.* 1987). Appreciable amounts of tapering have been reported to be evident for, at least, the terminal branches of dendritic trees (Ulfhake & Kellerth, 1981, 1983, 1984; Brown & Fyffe, 1981). In some studies, a pronounced tapering was also observed more proximally (Barrett & Crill, 1971, 1974). The calculated electrotonic distance

from soma to dendritic terminations has generally been found to vary over a relatively wide range within single dendritic trees (Barrett & Crill, 1974; Egger & Egger, 1982; Ulfhake & Kellerth, 1984; cf. also findings for brain stem motoneurones by Bras, Gogan & Tyc-Dumont, 1987). In view of all these differences between real motoneuronal dendritic trees and the requirements for the simple equivalent-cylinder model, we felt motivated to make an explicit analysis of one important aspect of the problem. Our question was: is the overall morphology of motoneuronal dendritic trees indeed such that their relative input conductance might be reasonably well predicted from measurements of their stem diameter? If so, would the relationship between stem diameter and input conductance resemble that of a uniform cylinder of finite length (i.e. input conductance proportional to stem diameter raised to the power of 3/2; cf. Rall, 1959, 1977)?

Some of the present findings have been briefly published as a congress abstract (Zwaagstra & Kernell, 1987).

METHODS

In the present study we made use of the same material as that of our preceding paper (Kernell & Zwaagstra, 1989). The analysis concerns fifty-two dendrites of four completely reconstructed motoneurones of m. triceps surae of adult cats. In order to facilitate the reading of the present paper, some general physiological and anatomical information from our companion paper is reproduced in Table 1 (Kernell & Zwaagstra, 1989). The neuronal input resistance of the motoneurones was measured over a range of weak injected currents using the spike-height method of Frank & Fuortes (1956; cf. Kernell, 1966; Lux *et al.* 1970; Kernell & Zwaagstra, 1981; Burke *et al.* 1982; Ulfhake & Kellerth, 1984).

For the purpose of the reconstruction and quantitative analysis, each dendritic tree was considered to consist of a series of *branches* which were limited by the soma–dendrite border, by points of division (branching) or by final termination. In producing the measurements, most branches were further subdivided into a sequence of consecutive *segments*. Each segment was measured with respect to its mean diameter and length, and these data were used for the calculations given below. At branch points, diameter measurements were taken from regions of a relatively constant thickness (i.e. outside the region of slight 'bulging' sometimes seen in the immediate proximity of the bifurcation itself). The size of the cell body was estimated on the basis of measurements of its transverse projection area in a reconstruction based on serial sections. From these measurements, its total surface area was computed according to the formula for a sphere (Table 1; Zwaagstra & Kernell, 1981). The stem dendrite diameter (e.g. Fig. 1, Table 1) was measured at a distance of 40 μm from the soma–dendrite border (or less if the first branch point occurred more proximally; Zwaagstra & Kernell, 1981; Kernell & Zwaagstra, 1989). The axon was not included in the present series of calculations.

Computations of electrical properties

For each dendritic tree, its expected electrical properties were analysed according to Rall (1959). In all the present calculations, dendritic end-branches were assumed to have sealed terminations (Rall, 1959). The expected input conductance of a dendrite (G_D) was obtained from the equation,

$$G_D = G_\infty B_0, \tag{1}$$

where G_∞ is the input conductance of an infinite cylinder of the same diameter as the proximal dendritic stem and B_0 is a weighting factor, calculated as described by Rall (1959). Dendritic size and branching pattern have a large influence on B_0. The value of G_∞ may be calculated from cylinder diameter d, membrane resistivity R_m and intracellular fluid resistivity R_i:

$$G_\infty = d^{3/2}\pi\,(4R_mR_i)^{-\frac{1}{2}}. \tag{2}$$

It was confirmed that, when applied to the test cases published by Rall (1959), our calculations gave the appropriate results.

When performing the calculations, all the dendrites of a given motoneurone were assumed to have uniform and equal membrane properties. R_i was assumed to be 70 Ω cm (Barrett & Crill, 1974). With respect to R_m, we used a number of alternative assumptions (see Results).

Unless otherwise noted, averages are given ±S.D.

TABLE 1. General properties of the reconstructed motoneurones

	Cell 3	Cell 1	Cell 4	Cell 2
Physiology				
Nerve	GL	G–sol	GM	G–sol
Axonal conduction velocity (m/s)	65	92	87	102
AHP duration (ms)	140	90	90	50
Input resistance (MΩ)	4·0	1·8	1·3	0·7
Anatomy				
Soma area (μm^2)	8576	8672	12336	15056
Number of dendritic trees	11	11	16	14
$\Sigma(D_s^{3/2})$ ($\mu m^{3/2}$)	242·4	267·1	400·4	426·8
Calculated				
'Own' membrane resistivity (kΩ cm^2)	15·9	5·4	4·3	1·8
D/S conductance ratio	45·4	33·6	26·8	16·8

Abbreviations: GL, gastrocnemius lateralis, G–sol, gastrocnemius–soleus, GM, gastrocnemius medialis; AHP, after-hyperpolarization. Soma area: total area of cell body, calculated as 4 times the soma area measured in transverse projection in reconstruction based on serial sections (Zwaagstra & Kernell, 1981). $\Sigma(D_s^{3/2})$: sum of dendritic stem diameters, raised to power of 3/2. 'Own' membrane resistivity: value of R_m calculated on basis of input resistance and detailed neuronal anatomy, assuming uniform membrane properties (see text). D/S conductance ratio: dendrite-to-soma conductance ratio as seen from the soma; calculated for uniform membrane properties. The neurones have been placed in an order of decreasing input resistance.

RESULTS

General properties of the reconstructed motoneurones

A number of general physiological and anatomical properties of the four reconstructed cells are shown in Table 1 (cf. Kernell & Zwaagstra, 1989). The four reconstructed cases were selected to represent as much as possible of the range of physiological properties of triceps surae motoneurones. Hence, the neuronal input resistance varied over a wide, nearly 6-fold range (Table 1).

Apparent membrane resistivity of the reconstructed motoneurones

For an initial series of calculations, we made the simplifying assumption that all membrane portions of a motoneurone had the same specific resistivity (see below and Table 3 for alternative assumptions). For each assumed value of such a uniform resistivity, the input conductance of every dendritic tree of the respective cell was calculated as described by Rall (1959; see Methods). The input conductance of the cell body was computed from its membrane surface area (Table 1; resistance of cytoplasm neglected). The input resistance of the whole cell was considered to be equal to the reciprocal value of the sum of the input conductances of its cell body and

that of all its dendrites (contribution of axon neglected). By repeating this procedure with different assumed values for R_m we ultimately found, by trial and error, the membrane resistivity that would produce a whole-cell input resistance equal to that measured experimentally (Rall, 1959; cf. Lux *et al.* 1970; Barrett & Crill, 1971, 1974; Ulfhake & Kellerth, 1984). In the remainder of the paper, these computed values of uniform resistivity will be referred to as the 'own' values of the respective cells.

The calculated 'own' values for uniform membrane resistivity spanned an almost 9-fold range, from 1·8 and 15·9 KΩ cm² (Table 1). There was a marked and statistically significant positive correlation between the calculated uniform mem-

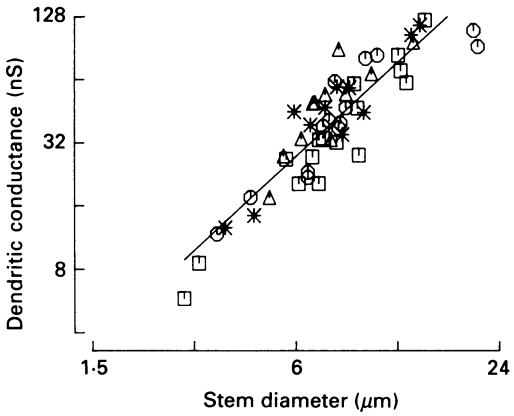

Fig. 1. Plot of computed dendritic input conductance (nS) *vs.* diameter of dendritic stems (μm). Stem diameters were measured at about 40 μm from the soma–dendrite border (Kernell & Zwaagstra, 1989). Logarithmic co-ordinates. Correlation coefficient $r = 0{\cdot}90$ ($P < 0{\cdot}001$). Regression line: $Y = 1{\cdot}49\,X + 0{\cdot}28$. For the calculations of this graph, all the fifty-two dendrites were assumed to have the same membrane resistivity (5 kΩ cm²).

brane resistivity and the measured input resistance ($r = +0{\cdot}9958$; $P < 0{\cdot}01$). Hence, among these cells, differences in membrane resistivity were apparently of major importance for the differences in neuronal input resistance (cf. Kernell & Zwaagstra, 1981; see Discussion for further comments).

Relation between dendritic stem diameter and calculated conductance

The double-logarithmic plot of Fig. 1 shows that there was a highly significant correlation between the computed value for dendritic input conductance (G_D; see Methods) and dendritic stem diameter (D_s). This was true for all the fifty-two dendrites taken together, as well as when performing the calculations separately for the dendrites of each neurone (Table 2; see also symbols for different cells in Fig. 1, Kernell & Zwaagstra, 1989). When calculated for each cell with its 'own' value of uniform membrane resistivity, the slope of the relation between log (G_D) and log (D_s) had an average value of 1·5 (range 1·25–1·63; Table 2). A slope of 1·5 was also obtained when the calculations were made for all fifty-two dendrites together (Fig. 1), and the value of this slope was markedly independent of the assumed value for

TABLE 2. Dendrite properties of the reconstructed motoneurones

	Cell 3	Cell 1	Cell 4	Cell 2
$\log(G_D)$ *vs.* log(stem diameter)				
Correlation coefficient	0·83	0·93	0·96	0·92
Mean slope	1·63	1·60	1·65	1·25
Range of slope (95% confidence)	0·81–2·45	1·14–2·06	1·37–1·93	0·91–1·59
*D*32 branch-point ratio				
Average	1·27±0·17	1·28±0·14	1·16±0·23	1·09±0·21
Variability (%)	38·1±15·3	33·5±6·6	34·1±18·0	34·2±13·6
Endings:				
Electrotonic distances				
Average	1·03±0·14	0·95±0·08	1·23±0·26	2·90±0·60
Variability (%)	22·3±11·0	31·5±10·8	32·6±12·3	33·2±12·1
Anatomical distances (mm)				
Average	1·22±0·12	0·71±0·04	0·82±0·17	1·02±0·19
Variability (%)	18·2±10·1	25·1±8·3	25·5±10·3	27·4±10·7

G_D: input conductance of dendritic tree, as seen from soma; calculations with 'own' value for R_m of each cell. Stem diameter: diameter of stem of dendritic tree. Mean slope: regression-slope coefficient for $\log(G_D)$ *vs.* log(stem diameter), as calculated separately for the dendrites of each cell (cf. Fig. 1). Range of slope: 95% confidence range for the respective regression coefficients. In the lower six data lines, means ±S.D. are given for measurements concerning the *D*32 branch-point ratio (cf. Fig. 3*A*) and for the electrotonic and anatomical distances to dendritic terminations. The *D*32 branch-point ratio was equal to the expression $\Sigma(d^{3/2})/D^{3/2})$, in which D is the diameter of a parent branch and d the diameters of its daughters. Electrotonic distances (anatomical distance/space constant) were calculated for each successive branch of a tree, using for each cell its 'own' value of membrane resistivity (Table 1). For each dendritic parameter, the mean ±S.D. is given for the average as well as for the variability (S.D./average) of measurements obtained for each one of the various dendrites.

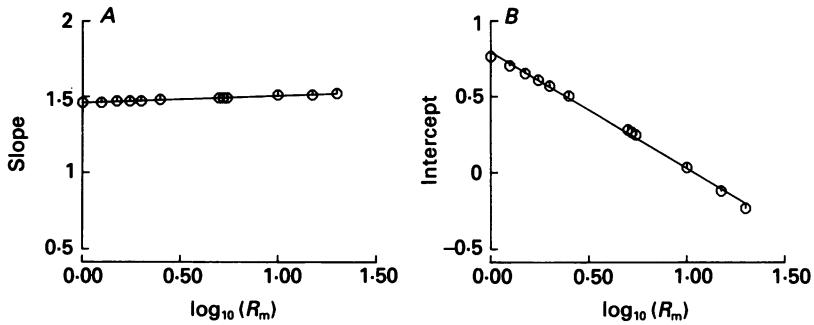

Fig. 2. Diagrams illustrating how changes in specific membrane resistivity (R_m) influenced the relation between dendritic input conductance (G_D) and dendritic stem diameter (D_s). This relationship could be expressed as $\log_{10}(G_D) = b \log_{10}(D_s) + a$ (cf. Fig. 1), where b is the slope and a is the Y-intercept of the regression line. The graphs show how this slope (*A*) and Y-intercept (*B*) were influenced when calculations for all fifty-two dendrites together were performed with different assumed values for R_m (kΩ cm²; plotted as logarithms). For *A*, the regression line was $Y = 0{\cdot}046\ X + 1{\cdot}46$ ($r = +0{\cdot}990$), and for *B* it was $Y = -0{\cdot}76\ X + 0{\cdot}79$ ($r = 0{\cdot}998$). In *B*, the Y-values are given in units of $\log_{10}$ (conductance in nS).

membrane resistivity (Fig. 2*A*). Hence, the relationship between dendritic input conductance and stem diameter would be approximated by:

$$\log_{10}(G_D) = 1{\cdot}5 \log_{10}(D_s) + a, \tag{3}$$

which may be rewritten as:

$$G_D = 10^a D_s^{3/2}. \tag{4}$$

As is demonstrated in Fig. 2*B*, the *y*-intercept *a* of eqn (3) varied markedly and linearly with the logarithm of membrane resistivity. The regression line of Fig. 2*B* has the equation,

$$a = -0{\cdot}76 \log_{10}(R_m) + 0{\cdot}794, \tag{5}$$

which may also be written as:

$$10^a = 10^{0{\cdot}794} R_m^{-0{\cdot}76}. \tag{6}$$

As $10^{0{\cdot}794}$ equals 6·22, eqn (4) may now be rewritten as:

$$G_D = D_s^{3/2} R_m^{-0{\cdot}76} 6{\cdot}22. \tag{7}$$

This equation summarizes our findings concerning the relationship between dendritic input conductance (nS), dendritic stem diameter (μm) and dendritic membrane resistivity (kΩ cm^2).

Comparisons between the reconstructed dendrites and ideal 'equivalent-cylinder dendrites'

According to the present results (Figs 1 and 2, eqn (7)), the calculated dendritic input conductance was proportional to the dendritic stem diameter raised to the power of 3/2. Thus, from this point of view, the reconstructed dendrites behaved very similarly to the class of equivalent-cylinder dendrites analysed by Rall (1959, 1977). From which other points of view did the reconstructed dendrites resemble or differ from Rall's equivalent-cylinder dendrites?

In an ideal equivalent-cylinder dendrite (see Introduction): (a) the '*D*32 branch-point ratio' should be equal to unity; (b) there should be no tapering; (c) all branch terminations should occur at the same electrotonic distance from the soma; and furthermore, (d) although it is not a necessary equivalent-cylinder requirement (Rall, 1977), model representations of dendritic trees are often drawn with a branching pattern that is symmetrically dichotomous (both daughters have the same diameter). Such a branch-point symmetry, if present, simplifies the quantitative analysis of a dendrite, partly because there will then be a closer correspondence between relative anatomical and electrotonic distances within the tree. The present reconstructed dendrites are analysed below with respect to points (a)–(d).

D32 branch-point ratio. This ratio showed a great deal of variation. When analysed for each dendritic tree separately, the index of variability (S.D./mean) was, on average, about 34% or more (Table 2). When comparing average values between the separate trees of a given motoneurone, the variability was about half as great, but still considerable (mean, 15·9% for the four neurones of Table 2). As is shown in

Fig. 3*A* and Table 2, the mean *D*32 branch-point ratio tended to be higher than unity for the present dendritic trees. This trend was statistically significant for all dendrites taken together (mean, 1·19±0·21) as well as, in three out of the four cases, for the dendrites of each neurone analysed separately (Table 2; *t* test for difference from 1·0 gave $P < 0{\cdot}02$ or less for all except cell 2). There was a slight but significant tendency for the mean *D*32 branch-point ratio to become somewhat greater at increasing somatofugal distances (Fig. 3*A*; $r = +0{\cdot}55$, $n = 16$, $P < 0{\cdot}05$; cf. Fig. 6*B* of Kernell & Zwaagstra, 1989).

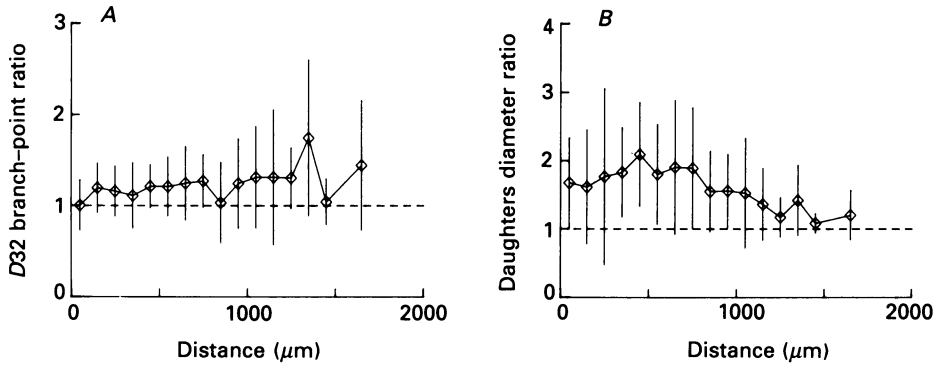

Fig. 3. Plots of mean dendritic branch-point properties (*Y* axis) *vs.* path distance from the soma–dendrite border (Distance). Plotted means ±S.D. calculated for the average values obtained per dendrite. *A*: '*D*32 branch-point ratio' is the expression $\Sigma(d^{3/2})/D^{3/2}$, as calculated for each individual branch point for parent (*D*) and daughter (*d*) dendrite diameters. *B*: 'Daughters diameter ratio' is the diameter ratio between the largest and smallest daughter branch, as calculated for each individual branch point. In *A* and *B*, distance bins with ⩽ 1 branch point were excluded; for plotted mean values, the number of cases (dendrites) was four or more.

Tapering. As mentioned already in our preceding paper (Kernell & Zwaagstra, 1989), the present dendrites often showed a significant amount of tapering. We estimated the average degree of such tapering to be around 12% per branch (Kernell & Zwaagstra, 1989). For further information on tapering, see below (section headed 'Combined effects of *D*32 branch-point ratio, tapering and distributed termination: '*D*32 stem ratio' *vs.* distance').

Distribution of dendritic terminations. As is demonstrated in Table 2, dendritic terminations were scattered over a considerable range of anatomical as well as electrotonic distances. When calculated separately for each individual dendritic tree, the mean variability in electrotonic distance to terminations was, for all dendrites together, about 30% (see Table 2 for values per cell). Thus, in this respect also the reconstructed dendrites clearly differed from the ideal equivalent-cylinder dendrite.

Symmetry of branching. There was a great degree of variability in symmetry of branching (cf. Fig. 3*B*). In general branching tended to be markedly asymmetric with respect to the diameters of sister branches (cf. Bras *et al.* 1987). There was a significant tendency for this asymmetry to become less marked at increasing somatofugal distances (Fig. 3*B*; $r = -0{\cdot}76$, $n = 16$, $P < 0{\cdot}001$). For all the dendrites and branch points taken together, the average ratio between the largest and smallest daughter diameter was 1·75.

Combined effects of D32 branch-point ratio, tapering and distributed termination: 'D32 stem ratio' vs. distance. In the ideal equivalent-cylinder dendrite, the expression Σ(branch diameter$^{3/2}$) would retain a constant value at all electrotonic distances from the cell body. This would also be true for all anatomical distances, provided that none of the branches terminated (termination would happen at different anatomical distances for branches of the same electrotonic length if they differed in diameter). Hence, in cases behaving like the ideal equivalent-cylinder model, the ratio Σ(branch diameter$^{3/2}$)/(stem diameter$^{3/2}$) (i.e. the *D*32 stem ratio) would remain at a value of 1·0 for all somatofugal distances until the various branches terminated.

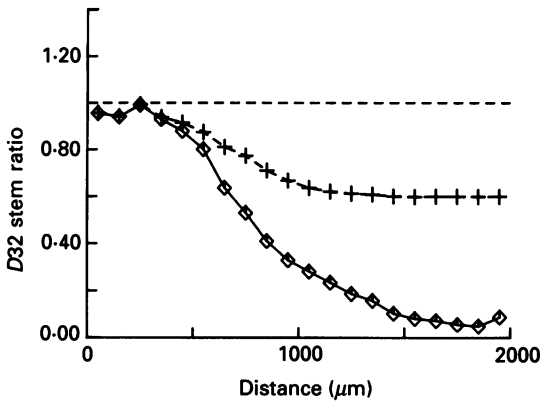

Fig. 4. Plot illustrating how the '*D*32 stem ratio' (*Y*-axis) of dendritic trees varied with distance from the soma (μm). The *D*32 stem ratio was equal to $\Sigma(d^{3/2})/D_s^{3/2}$, where d was the dendritic segment diameter at a given somatofugal distance and D_s was the diameter of the corresponding dendritic stem. The plotted means were calculated from the average values obtained per dendrite for all the reconstructed trees together (◇). The crosses show the same relationship under the assumed condition that none of the dendritic branches terminated; in this case all branches were assumed to continue to infinite length with the diameter measured just prior to termination. In order to facilitate analysis of the plot, a dashed line has been drawn for a *D*32 stem ratio of 1·0. In an ideal equivalent-cylinder dendrite, all the values should have followed this line (Rall, 1959, 1977). Values of *D*32 stem ratio became significantly different from 1·0 at distances exceeding 400 μm (*t* test).

The diagram of Fig. 4 shows that, for all the present dendrites analysed together, the average *D*32 stem ratio remained reasonably close to 1·0 over the initial 400–500 μm (average not significantly different from 1·0 at $\leqslant 400$ μm). Thus, for these moderate somatofugal distances, there was apparently a balance between the effects of tapering and the effects of the relatively large *D*32 branch-point ratio (cf. Fig. 3*A*). At somatofugal distances of about 500–1500 μm there was a progressive and continuous decline in the average *D*32 stem ratio. In Fig. 4, the upper curve (+) corresponds to the *D*32 stem ratio that would be obtained if none of the branches ever terminated (cf. Ulfhake & Kellerth, 1981; Rose, Keirstead & Vanner, 1985). Hence, this upper curve represents the isolated effect of net changes in branch diameter on the *D*32 stem ratio (summed effects of tapering and *D*32 branch-point ratios), and the difference between the upper and lower curves represents the relative effect of branch termination. The average results of Fig. 4 indicate that, at least over an intermediate range of distances (about 500–1000 μm), the decline in *D*32 stem ratio was caused by diameter decline as well as by branch termination.

The data of Fig. 4 show averages for mean values obtained from each one of the present fifty-two dendrites. When the corresponding types of measurement were plotted separately for the dendrites of each cell (Fig. 5), the results indicated that individual motoneurones may show distinct differences with respect to the manner in which their *D*32 stem ratio declines with somatofugal distance. In the two cells with the highest input resistance, the *D*32 stem ratio even seemed to show an initial overshoot to values above 1·0 (Fig. 5, cells 3 and 1). A similar tendency was recently described for slow-twitch motoneurones in the study of Cullheim *et al.* (1987). In the

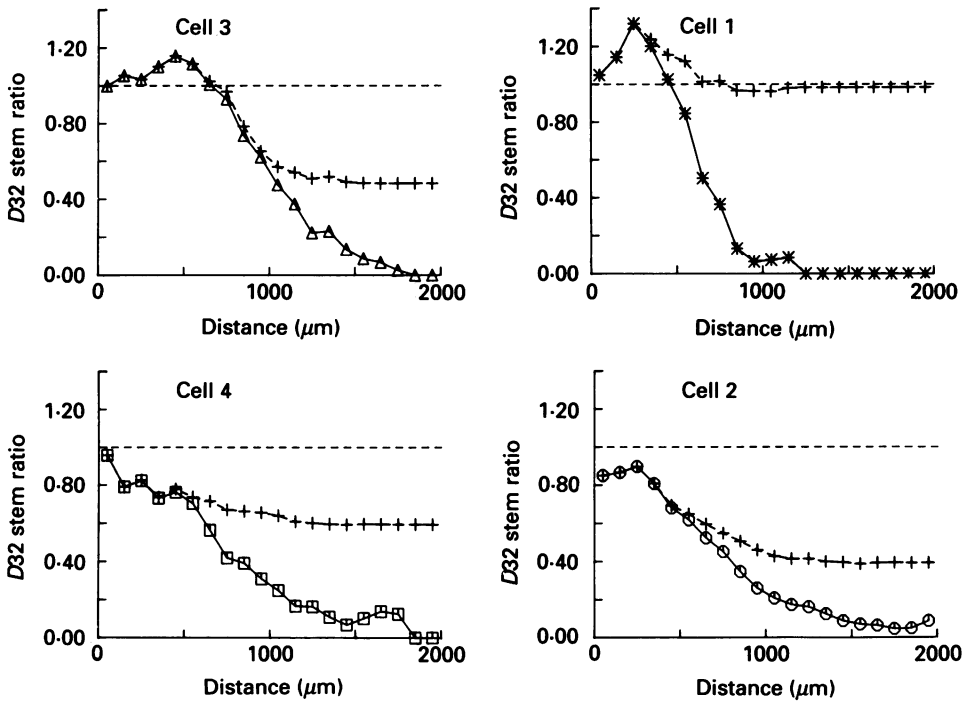

Fig. 5. Plots like that of Fig. 4, but for values calculated separately for the dendrites of each reconstructed neurone. The cells have been arranged in order of decreasing input resistance (cf. Tables 1–3). Values of *D*32 stem ratio became significantly different from 1·0 at distances exceeding 600 μm (cell 1), 300 μm (cell 2), 800 μm (cell 3) and 100 μm (cell 4).

present case, however, none of the apparent 'overshoot values' were significantly greater than unity (*t* test, $P > 0{\cdot}05$). The present number of cells is too small for any general conclusion concerning the possible relation between the decline of *D*32 stem ratio and other neuronal properties.

Effects of differences in membrane resistivity between soma and dendrites

The calculations of the 'own' membrane resistivity of the present motoneurones (Table 1) were performed on the assumption that the membrane of the soma had the same passive properties as that of the dendrites. If this was the case, the neuronal input conductance would largely be determined by the resting properties of

its dendritic membrane (large dendrite-to-soma conductance ratio; see last line of Table 1).

In order to explore some of the effects of differences between the somatic and dendritic membrane resistivity, we performed a number of additional calculations for which some results are displayed in Table 3. In these cases, the input conductance of each dendritic tree was computed from its stem diameter using eqn (7). A proportionality factor was assumed for the ratio between dendritic and somatic resistivity. Given this assumption, resistivity values were computed that would produce a neuronal input resistance equal to that measured experimentally (cf. Table 1).

TABLE 3. Predicted electrical cell properties for different degrees of inhomogeneity between soma and dendrite membranes

	Cell 3	Cell 1	Cell 4	Cell 2
Dendr. R_m = 35 × soma R_m				
Soma R_m (Ω cm^2)	716	308	325	198
D/S conductance ratio	1·09	0·97	1·03	0·87
Dendr. R_m = 500 × soma R_m				
Soma R_m (Ω cm^2)	386	174	180	115
D/S conductance ratio	0·12	0·11	0·12	0·09

Dendr. R_m: resistivity of dendritic membrane. Soma R_m: resistivity of soma membrane. D/S conductance ratio: cf. Table 1. Tabulated values calculated using eqn (7) and measurements of $\Sigma(D_s^{3/2})$ and soma area (cf. Table 1). See text for further explanation.

For a dendritic resistivity of 35 times that of the soma, the dendrite-to-soma conductance ratio was close to 1·0 (Table 3). Thus, in this case the dendritic and somatic membranes were of about equal importance for determining the total neuronal input resistance. For a dendritic resistivity of 500 times that of the soma (cf. Clements & Redman, 1986; Glenn *et al.* 1987), the dendritic input conductance would be only about 10% of that of the soma. In this case, the cellular input conductance would clearly be dominated by the properties of its somatic membrane.

For all the conditions shown in Table 3, there was a statistically significant correlation between the measured neuronal input resistance and the required membrane resistivity (somatic or dendritic; $r \geqslant +0{\cdot}98$, $P < 0{\cdot}05$).

DISCUSSION

A major result of the present study is summarized in eqn (7), which shows how the approximate dendritic input conductance of triceps surae motoneurones might be calculated from measurements of their dendritic stem diameter and an assumed value for dendritic membrane resistivity.

In a preceding study, we used more restricted anatomical reconstructions for analysing the relationship between size and input resistance among cat's hindlimb motoneurones. We then concluded that the differences in neuronal size were far too small to be responsible for the measured differences in neuronal input resistance (Kernell & Zwaagstra, 1981). Hence, we also concluded that the differences in

motoneuronal input resistance between high- *vs.* low-resistance cells (or slow-axoned *vs.* fast-axoned cells) were to an important degree caused by differences in specific membrane resistivity (see also Burke *et al.* 1982; Ulfhake & Kellerth, 1984; Gustafsson & Pinter, 1984). This conclusion receives further support from the results of the present study. Firstly, the argument of Kernell & Zwaagstra (1981) was partly based on the assumption that dendritic input conductance would be proportional to the 3/2 power of dendritic stem diameter. This assumption is completely in accordance with the present experimental findings (eqn (7), Figs 1 and 2*A*, Table 2). Secondly, although our present number of neurones is small, the results from these four cells provide direct evidence that differences in input resistance between motoneurones are, to a great extent, caused by differences in membrane resistivity (cf. Table 1). As we pointed out in our previous study (Kernell & Zwaagstra, 1981), differences in membrane resistivity are likely to be of great importance for the way in which the various motoneurones will be recruited in postural control and movement.

In a number of ways, the properties of the present motoneuronal dendrites clearly deviated from those of the ideal equivalent-cylinder dendrites described by Rall (1959, 1977): (a) the '*D*32 branch-point ratio' tended to be greater than unity (Table 2, Fig. 3*A*); (b) there was tapering (Fig. 4; cf. Kernell & Zwaagstra, 1989); (c) the various end-branches of a given tree did not terminate at the same electrotonic distance from the cell body (see Table 2).

All these kinds of deviations from the ideal equivalent-cylinder model have also been noted by various preceding investigators (see Introduction). In spite of these deviations, the present motoneuronal dendrites resembled those of the ideal equivalent-cylinder model with respect to the relationship between stem diameter and calculated input conductance: in both cases, input conductance was proportional to the 3/2 power of stem diameter (cf. eqn (7)). This model-like behaviour was apparently partly due to the fact that various non-model-like properties of the neuronal dendrites tended to balance each other. Particularly within the most proximal portions of the tree, the relatively great *D*32 branch-point ratio (Table 2, Fig. 3*A*) tended to become balanced by dendritic tapering (cf. Fig. 4). As a result, the *D*32 stem ratio, as obtained for the whole material together, remained close to unity during several hundred microns. The proximal portions of the dendrites would, of course, be those most important for dendritic input conductance as seen from the soma.

A *D*32 stem ratio similar to that of Fig. 4, remaining close to unity over initial somatofugal distances of several hundred microns, has been reported in several previous investigations of hindlimb motoneurones (Ulfhake & Kellerth, 1981, 1983; Cullheim *et al.* 1987). In some other cases, a continuous decline of *D*32 stem ratio was found to be the most typical pattern (Barrett & Crill, 1971, 1974; Egger & Egger, 1982). The latter type of behaviour resembles that of our cell 4 (Fig. 5).

In addition to the relationship between dendritic input conductance and stem diameter, our results also showed that the computed dendritic input conductance tended to be proportional to membrane resistivity raised to the power of $-0{\cdot}76$ (see eqn (7)). If all dendrites had had an infinite electrotonic length, dendritic input conductance would have been proportional to membrane resistivity raised to the

power of −0·5 (see eqns (1) and (2)). For equivalent-cylinder models, however, a slope more negative than −0·5 would be obtained for a population of dendrites of a finite electrotonic length and a fixed anatomical length. We performed control calculations with uniform cylinders of a diameter equal to that of an average dendritic stem (8·4 μm). If these cylinders had a length of about 1·2 mm, then the relation between log (G_D) and log (R_m) had a slope of about −0·75 (correlation coefficient $r = +0{\cdot}99$).

As calculated for uniform properties of the soma–dendritic membrane, the present values of specific membrane resistivity (1·8, 4·3, 5·4, 15·9 kΩ cm^2; Table 1) overlap with, but tend to be higher than, estimates obtained by similar techniques in previous investigations (Lux *et al.* 1970: 1·5–4·1 kΩ cm^2; Barrett & Crill, 1974: 1·3–3·6 kΩ cm^2 when maximally compensated for possible incompleteness of staining of terminal endings; Ulfhake & Kellerth, 1984: 0·75 and 2·0 kΩ cm^2). These differences might partly reflect sampling variations. Our estimates of mean electrotonic length (1·0, 1·0, 1·2, 2·9 space constants; Table 2) also overlap with those of earlier electroanatomical studies (Lux *et al.*, 1970: 1·2–2·0 space constants; Barrett & Crill, 1974: 1·1–1·5 space constants; Ulfhake & Kellerth, 1984: 2·8 and 4·6 space constants).

It is also of some interest to compare the present calculated cell properties for uniform membrane properties (Tables 1 and 2) with corresponding data from electrophysiological experiments; the measurements concerned were done according to procedures appropriate for uniform equivalent-cylinder models of motoneurones (Rall, 1977). Such experimental determinations of membrane time constant have shown values in the range of 2–10 (sometimes to 14) ms (Nelson & Lux, 1970; Lux *et al.* 1970; Burke & ten Bruggencate, 1971; Jack, Miller, Porter & Redman, 1971; Iansek & Redman, 1973; Barrett & Crill, 1974; Gustafsson & Pinter, 1984; Ulfhake & Kellerth, 1984; values up to about 14 ms: Zengel, Reid, Sypert & Munson, 1985). That fits fairly well with the membrane time constants that one would obtain for the presently reconstructed cells with their 'own' membrane resistivity and a normal specific membrane capacitance of 1 μF/cm^2 (about 2, 4, 5 and 16 ms; cf. Table 1). Electrophysiological estimates of electrotonic length for whole motoneurones have usually given values in the range of 1–2 space constants (Nelson & Lux, 1970; Lux *et al.* 1970; Burke & ten Bruggencate, 1971; Jack *et al.* 1971; Iansek & Redman, 1973; Gustafsson & Pinter, 1984; Ulfhake & Kellerth, 1984). Our estimates of average electrotonic distance to dendritic terminations fall within this range for the present cells 1, 3 and 4, whereas the mean value was as great as 2·9 space constants for cell 2 (Table 2). It should be noted, however, that commonly used methods for electrophysiological estimates of electrotonic length will not give accurate results at long real lengths (Rall, 1977); great uncertainties may be expected for real lengths exceeding about 1·5–2 space constants (de Jongh & Kernell, 1982). Electrophysiological estimates of dendrite *vs.* soma conductance ratios have usually suggested ratios in excess of 5, which is consistent with the values of Table 1. However, the available electrophysiological methods have usually been considered to give rather uncertain and highly approximate results (Nelson & Lux, 1970; Jack *et al.* 1971; Iansek & Redman, 1973; Ulfhake & Kellerth, 1984).

There is increasing evidence suggesting that, at least under normal experimental

circumstances (microelectrode in cell body), the membrane resistivity might be higher for the dendrites than for the soma (Iansek & Redman, 1973; Fleshman *et al.* 1983; Ulfhake & Kellerth, 1984; Clements & Redman, 1986; Glenn *et al.* 1987; cf. also Barrett & Crill, 1974). Thus, the present estimates of the 'own' uniform membrane resistivity of the various motoneurones may be too high for the soma and too low for the dendrites (Table 1; see Table 3 for alternative values of membrane resistivity and dendrite *vs.* soma conductance ratio). As a consequence, the mean electrotonic length of the dendrites might in reality be shorter than those given in Table 2. These considerations are not, however, of paramount importance in relation to the main question of the present analysis, which concerns relative comparisons between dendrites and motoneurones rather than their absolute membrane properties.

REFERENCES

Barrett, J. N. & Crill, W. E. (1971). Specific membrane resistivity of dye-injected cat motoneurons. *Brain Research* **28**, 556–561.

Barrett, J. N. & Crill, W. E. (1974). Specific membrane properties of cat motoneurones. *Journal of Physiology* **239**, 301–324.

Bras, H., Gogan, P. & Tyc-Dumont, S. (1987). The dendrites of single brain-stem motoneurons intracellularly labelled with horseradish peroxidase in the cat. Morphological and electrical differences. *Neuroscience* **22**, 947–970.

Brown, A. G. & Fyffe, R. E. W. (1981). Direct observations on the contacts made between Ia afferent fibres and α-motoneurones in the cat's lumbosacral spinal cord. *Journal of Physiology* **313**, 121–140.

Burke, R. E. (1981). Motor units: anatomy, physiology and functional organization. In *Handbook of Physiology – The Nervous System II*, part 1, ed. Brooks, V. B., pp. 345–422. Bethesda, MD, USA: American Physiological Society.

Burke, R. E., Dum, R. P., Fleshman, J. W., Glenn, L. L., Lev-Tov, A., O'Donovan, M. J. & Pinter, M. J. (1982). An HRP study of the relation between cell size and motor unit type in cat ankle extensor motoneurons. *Journal of Comparative Neurology* **209**, 17–28.

Burke, R. E. & ten Bruggencate, G. (1971). Electrotonic characteristics of alpha motoneurones of varying size. *Journal of Physiology* **212**, 1–20.

Clements, J. D. & Redman, S. J. (1986). Electrical and geometrical non-uniformities in motoneurone cable properties. *Neuroscience Abstracts* **12**, 851.

Cullheim, S., Fleshman, J. W., Glenn, L. L. & Burke, R. E. (1987). Membrane area and dendritic structure in type-identified triceps surae alpha-motoneurons. *Journal of Comparative Neurology* **255**, 68–81.

de Jongh, H. R. & Kernell, D. (1982). Limits of usefulness of electrophysiological methods for estimating dendritic length in neurones. *Journal of Neuroscience Methods* **6**, 129–138.

Egger, M. D. & Egger, L. D. (1982). Quantitative morphological analysis of spinal motoneurons. *Brain Research* **253**, 19–30.

Fleshman, J. W., Segev, I., Cullheim, S. & Burke, R. E. (1983). Matching electrophysiological with morphological measurements in cat α-motoneurons. *Neuroscience Abstracts* **9**, 341.

Frank, K. & Fuortes, M. G. F. (1956). Stimulation of spinal motoneurones with intracellular electrodes. *Journal of Physiology* **134**, 451–470.

Glenn, L. L., Samojla, B. G. & Whitney, J. F. (1987). Electrotonic parameters of cat spinal α-motoneurons evaluated with an equivalent cylinder model that incorporates non-uniform membrane resistivity. *Brain Research* **435**, 398–402.

Gustafsson, B. & Pinter, M. J. (1984). Relations among passive electrical properties of lumbar α-motoneurones of the cat. *Journal of Physiology* **356**, 401–431.

Iansek, R. & Redman, S. J. (1973). An analysis of the cable properties of spinal motoneurones using a brief intracellular current pulse. *Journal of Physiology* **234**, 613–636.

JACK, J. J. B., MILLER, S., PORTER, R. & REDMAN, S. J. (1971). The time course of minimal excitatory post-synaptic potentials evoked in spinal motoneurones by group Ia afferent fibres. *Journal of Physiology* **215**, 353–380.

KERNELL, D. (1966). Input resistance, electrical excitability, and size of ventral horn cells in cat spinal cord. *Science* **152**, 1637–1640.

KERNELL, D. & ZWAAGSTRA, B. (1981). Input conductance, axonal conduction velocity and cell size among hindlimb motoneurones of the cat. *Brain Research* **204**, 311–326.

KERNELL, D. & ZWAAGSTRA, B. (1989). Size and remoteness: two relatively independent parameters of dendrites, as studied for spinal motoneurones of the cat. *Journal of Physiology* **413**, 233–254.

LUX, H. D., SCHUBERT, P. & KREUTZBERG, G. W. (1970). Direct matching of morphological and electrophysiological data in cat spinal motoneurones. In *Excitatory Synaptic Mechanisms*. ed. ANDERSEN, P. & JANSEN, J. K. S., pp. 189–198. Oslo: Universitetsforlaget.

NELSON, P. G. & LUX, H. D. (1970). Some electrical measurements of motoneuron parameters. *Biophysical Journal* **10**, 55–73.

RALL, W. (1959). Branching dendritic trees and motoneuron membrane resistivity. *Experimental Neurology* **1**, 491–527.

RALL, W. (1977). Core conductor theory and cable properties of neurons. In *Handbook of Physiology – The Nervous System I*, Part 1, ed. KANDEL, E., pp. 39–97. Bethesda, MD, USA: American Physiological Society.

ROSE, P. K., KEIRSTEAD, S. A. & VANNER, S. J. (1985). A quantitative analysis of the geometry of cat motoneurons innervating neck and shoulder muscles. *Journal of Comparative Neurology* **239**, 89–107.

ULFHAKE, B. & KELLERTH, J.-O. (1981). A quantitative light microscopic study of the dendrites of cat spinal α-motoneurons after intracellular staining with horseradish peroxidase. *Journal of Comparative Neurology* **202**, 571–583.

ULFHAKE, B. & KELLERTH, J.-O. (1983). A quantitative morphological study of HRP-labelled cat α-motoneurones supplying different hindlimb muscles. *Brain Research* **264**, 1–19.

ULFHAKE, B. & KELLERTH, J.-O. (1984). Electrophysiological and morphological measurements in cat gastrocnemius and soleus α-motoneurones. *Brain Research* **307**, 167–179.

ZENGEL, J. E., REID, S. A., SYPERT, G. W. & MUNSON, J. B. (1985). Membrane electrical properties and prediction of motor-unit type of medial gastrocnemius motoneurons in the cat. *Journal of Neurophysiology* **53**, 1323–1344.

ZWAAGSTRA, B. & KERNELL, D. (1981). Sizes of soma and stem dendrites in intracellularly labelled α-motoneurones of the cat. *Brain Research* **204**, 295–309.

ZWAAGSTRA, B. & KERNELL, D. (1987). Relationship between predicted input conductance and stem diameter in dendrites of cat's spinal motoneurones. *Neuroscience, suppl.*, **22**, S793.